

Lawrence Berkeley National Laboratory

Lawrence Berkeley National Laboratory

Title

A Novel Semi-biosynthetic Route for Artemisinin Production Using Engineered Substrate-Promiscuous P450BM3

Permalink

<https://escholarship.org/uc/item/1q7036nj>

Author

Dietrich, Jeffrey

Publication Date

2009-03-09

Peer reviewed

A Novel Semi-biosynthetic Route for Artemisinin Production Using Engineered Substrate-Promiscuous P450_{BM3}

Jeffrey A. Dietrich^{†,¶,‡,§}, Yasuo Yoshikuni^{†,¶,‡,§}, Karl J. Fisher[#], Frank X. Woolard[#], Denise Ockey[#], Derek J. McPhee[#], Neil S. Renninger[#], Michelle C. Y. Chang^{¶,‡}, David Baker^{‡,ü}, and Jay D. Keasling^{†,¶,§,††,*}

[†]UCSF/UCB Joint Graduate Group in Bioengineering, [‡]California Institute for Quantitative Biomedical Research (QB3),

[!]Department of Chemistry, and [§]Department of Chemical Engineering, University of California at Berkeley, Berkeley,

California 94720, [¶]Synthetic Biology Department, Physical Biosciences Division, Lawrence Berkeley National Laboratory,

Berkeley, California 94710, [‡]Department of Biochemistry, University of Washington, Seattle, Washington 98195, ^üHoward

Hughes Medical Institute, Seattle, Washington 98195, [#]Amyris Biotechnologies Inc., Emeryville, California 94208, and ^{††}Joint

BioEnergy Institute, Emeryville, California 94208. ^{‡‡}These authors contributed equally to this work. ^{§§}Present address: Bio

Architecture Lab, Inc., Seattle, Washington 98103.

ABSTRACT

Production of fine heterologous pathways in microbial hosts is frequently hindered by insufficient knowledge of the native metabolic pathway and its cognate enzymes; often the pathway is unresolved and enzymes lack detailed characterization. An alternative paradigm to using native pathways is *de novo* pathway design using well-characterized, substrate-promiscuous enzymes. We demonstrate this concept using P450_{BM3} from *Bacillus megaterium*. Using a computer model, we illustrate how key P450_{BM3} active site mutations enable binding of non-native substrate amorphadiene, incorporating these mutations into P450_{BM3} enabled the selective oxidation of amorphadiene artemisinic-11 α ,12-epoxide, at titers of 250 mg L⁻¹ in *E. coli*. We also demonstrate high-yielding, selective transformations to dihydroartemisinic acid, the immediate precursor to the high value anti-malarial drug artemisinin.

Engineering biosynthetic pathways for low-cost production of fine chemicals is becoming an increasingly attractive alternative to synthetic chemistry routes. In many cases, however, an enzyme in the desired native pathway is missing or difficult to functionally express in a heterologous host, leading to low product yields. An alternative paradigm to using native pathways and their cognate enzymes is *de novo* pathway construction through incorporation of engineered substrate-promiscuous enzymes—enzymes capable of acting upon a broad range of substrates. Substrate promiscuities are believed to be hallmark characteristics of primitive enzymes, serving as evolutionary starting points from which greater specificity is acquired following application of selective pressures (1-3). In this respect, substrate-promiscuous enzymes are logical starting points for *de novo* metabolic pathway design. This process functionally mimics one method for how nature is believed to evolve novel biosynthetic routes. Following demonstration of a desired enzyme activity, computational, rational, or directed evolution engineering strategies can further tailor a promiscuous enzyme toward greater specificity.

As an example of using substrate-promiscuous enzymes in engineered biosynthetic pathways, we sought to develop a novel semi-biosynthetic route for production of the sesquiterpene lactone endoperoxide artemisinin. Naturally derived from the plant *Artemisia annua*, artemisinin is a highly important antimalarial pharmaceutical. Artemisinin-based combination therapies (ACTs) are currently being recommended by the World Health Organization as the first-line malaria treatment (4). However, under the production regime in which artemisinin is harvested from natural sources, ACTs are 10–20 times more expensive than existing alternatives (5). Paucity of supply and high cost currently make ACTs prohibitively expensive in areas to which malaria is endemic. In light of this and other difficulties, malaria remains one of the most debilitating and prevalent infectious diseases; between 300 and 500 million people are infected annually, resulting in more than 1 million deaths (6). High-level production of a precursor to artemisinin in a microbial host could significantly reduce production costs and enable broader distribution of ACTs. Although there exist multiple routes for both the complete and partial chemical synthesis of artemisinin (7), they are all too low-yielding and complicated to enable production of low-cost artemisinin. When examining the native artemisinin biosynthetic

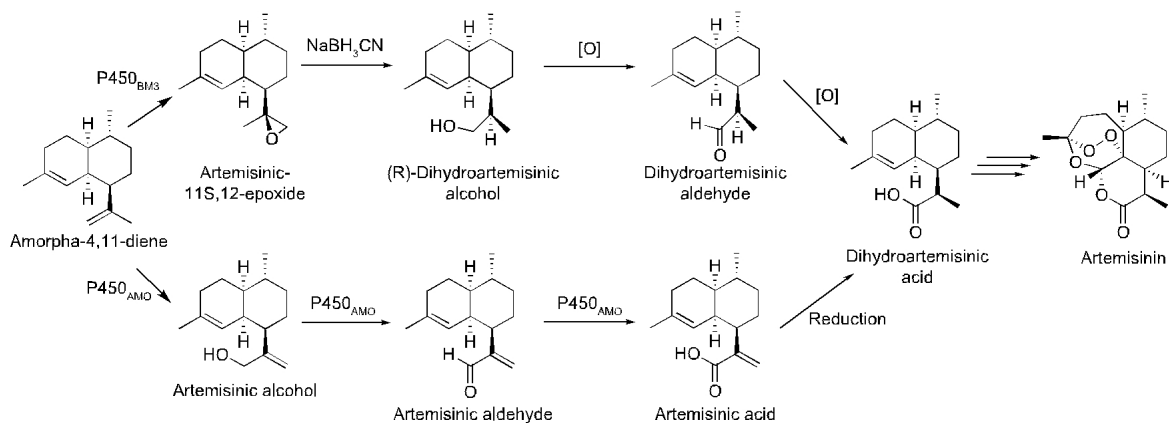
route, two distinct challenges emerge: syn-thesis of the complicated terpene olefin pre-cursor, amorphadiene, and selective oxida-tion and reduction of amorphadiene to produce dihydroartemisinic acid (Scheme 1). Dihydroartemisinic acid is the immedi-ate precursor to artemisinin and has been shown to be readily transformed (8, 9). The first complication can be overcome by pro-ducing amorphadiene microbially. To this end, we have previously engineered both *Escherichia coli* and *Saccharomyces cerevisiae* for the high-level production of amorph-adiene (10–13).

Selective oxidation and reduction of the undecorated amorphadiene skeleton re-mains a difficult task. There exist multiple routes for oxidizing amorphadiene: chemi-cal oxidations, biological oxidations using native enzymes, or biological oxidations us-ing non-native enzymes. Oxidation of amorphadiene using chemical catalysts poses numerous problems, including high expense, low product yield, and poor regio- and stereoselectivity (7, 14). Use of the na-tive *A. annua* cytochrome P450 monooxyge-nase (CYP71AV1, referred to herein as P450AMO) and oxidoreductase provides a biological alternative to chemical synthesis. Compared to synthetic chemistry-based oxi-dations, biocatalyst-based approaches are often able to circumvent problems with regio- and stereoselectivity pervasive to syn-thetic chemistry (15, 16). However, eukary-otic P450s have their own share of difficul-ties and are notoriously problematic to express in heterologous hosts such as *E. coli*. Difficulties with protein–membrane association, folding, post-translational modification, and cofactor integration all hinder successful integration of native en-zymes into heterologous pathways ex-pressed in *E. coli* (17). Although we previ-ously engineered both *E. coli* and *S. cerevisiae* for production of artemisinic acid (13, 18), *E. coli* cultures harboring the P450AMO-catalyzed biosynthetic route exhibit numer-ous handicaps. Mixed oxidation products with a relatively low artemisinic acid yield (>100 mg L⁻¹), 7-day culture periods at 20 °C to obtain functional P450AMO activity, and the need for selective reduction of the terminal olefin to produce dihydroartemis-inic acid all inhibit industrial scale-up of this route. In particular, selective reduction of amorphadiene’s terminal olefin over the en-docyclic olefin using synthetic chemistry is difficult to achieve at high yields (19, 20).

Here we demonstrate an alternate semi-biosynthetic route, producing dihydroarte-misinic acid using an engineered substrate-promiscuous P450BM3 in conjunction with high-yielding, selective synthetic chemistry. We selected P450BM3 derived from *Bacillus megaterium* for this study. Wild-type P450BM3 is known to catalyze the hydroxyla-tion of long chain, saturated fatty acids. P450BM3 possesses the highest turnover rate of any known P450, approaching 17,000 min⁻¹ in the case of arachidonate (21), and has a demonstrated capacity to be re-engineered (22–24).

Minimizing the number of side reactions and products is a difficult task when re-engineering enzymes for non-native sub-strates but is a near requirement in meta-bolic engineering applications. In the case of P450BM3, when using amorphadiene as a substrate we believed that the lower transi-tion state energy of CAC epoxidation com-pared to C–H hydroxylation would favor pro-duction of a few, or at best one, product species. Artemisinic-11S,12-epoxide (arte-misinic epoxide), the result of terminal ole-fin oxidation, could serve as an intermediate in our novel semi-biosynthetic route toward artemisinin (Scheme 1). Epoxide cleavage to form dihydroartemisinic alcohol necessitates two oxidations that are not required in the native biosynthetic pathway to form dihydroartemisinic acid; however, this route negates the need for the difficult regioselective reduction of the terminal olefin of artemisinic acid to form dihydroartemisinic acid, as is required when using P450_{AMO}.

SCHEME 1. Semi-biosynthetic strategies for production of artemisinina



^aA comparison of the routes catalyzed by P450_{AMO} and P450_{BM3} for the production of dihydroartemisinic acid, from which artemisinin can be readily synthesized. Both routes necessitate additional synthetic chemistry following P450-catalyzed functionalization of amorphadiene.

TABLE 1. Amorphadiene epoxidation rates of P450_{BM3} variants^a

P450 _{BM3} variant	NADPH consumption rate	Amorphadiene epoxidation rate	Coupling (%)
WT	N.D.	N.D.	N.D.
G1	22.20 ± 4.10	7.77 ± 1.4	35
G3	48.23 ± 3.61	30.38 ± 2.27	63
G4	60.90 ± 3.84	30.45 ± 3.84	50

^aNADPH consumption rates and amorphadiene epoxidation rates are given in nmol (nmol P450)⁻¹ min⁻¹ (mean ± SD, n = 3). Coupling is the ratio of the amorphadiene epoxidation rate to the NADPH consumption rate. No epoxidation of amorphadiene was detected using wild-type P450_{BM3}. Observed increases in amorphadiene epoxidation rates between G1 and G3 match well with *in vivo* production data; G4 exhibited a NADPH consumption rate higher than that of G3, but this did not manifest itself as a higher amorphadiene oxidation rate. This may be explained, in part, by the low coupling efficiency measured *in vitro* for variant G4.

Technical feasibility of our proposed synthetic chemistry steps was demonstrated by conversion of artemisinic epoxide to dihydroartemisinic acid. First, artemisinic acid was reduced to dihydroartemisinic alcohol (81% yield based on reacted epoxide); subsequently, dihydroartemisinic alcohol was oxidized to dihydroartemisinic aldehyde and dihydroartemisinic acid with yields of 76% and 78%, respectively. Identification of the intermediates along the above route was confirmed by gas chromatography/mass spectrometry (GC/MS) and ¹H NMR spectrometry comparison to both an authentic standard and published results (25, 26). The yields witnessed at the bench scale indicate our proposed synthetic route is competitive with the native P450_{AMO}-catalyzed route for artemisinin production.

The initial overexpression of wild-type P450_{BM3} in *E. coli* engineered to produce amorphadiene demonstrated no detectable oxidation activity toward the substrate as indicated by GC/MS analysis. Purified

wild-type enzyme also did not show any detectable activity during *in vitro* assays using amorphadiene as a substrate (Table 1). A model structure of the lowest energy transition state complex for amorphadiene in the P450_{BM3} active site was created using ROSETTA-based energy minimization (27). This model clearly illustrates the steric hindrance imposed on amorphadiene by residue Phe87 in the wild-type enzyme

(Figure 1). This analysis was supported by previous work demonstrating that mutations at position Phe87 strongly dictate alternate substrate promiscuity (21, 23, 24).

Our first goal was to increase the size of the active site binding pocket, which we believed would impart broad substrate promiscuity on P450_{BM3}. To this end, we incorporated mutation F87A into the wild-type enzyme (referred to as G1 herein). *E. coli* engineered to produce amorphadiene and harboring P450_{BM3} variant G1 produced a single compound exhibiting a retention time and electron-impact (EI) mass spectrum entical to those of an artemisinic epoxide standard when analyzed by GC/MS (Supplementary Figure 1) (14).

While the promiscuity of P450_{BM3} variant G1 enabled production of our desired product, the *in vivo* expression of this enzyme could potentially have the negative effect of oxidizing a wide range of intracellular metabolites. Fatty acids, the native substrates for wild-type P450_{BM3}, were identified as the most likely intracellular candidates for oxidation. In an attempt to address this issue, we created an additional variant containing the mutations G1!R47L/Y51F (referred to herein as G3). Residues Arg47 and Tyr51 are found along the entrance of the substrate access channel. These residues interact with the carboxy group of fatty acids, stabilizing the molecule in the channel during oxidation, and the combination of both mutations has been demonstrated to greatly reduce fatty acid oxidation (28). We hypothesized the incorporation of P450_{BM3} variant

G3 into our biosynthetic pathway would increase product titers as a result of the elimination of potential sources of competitive inhibition.

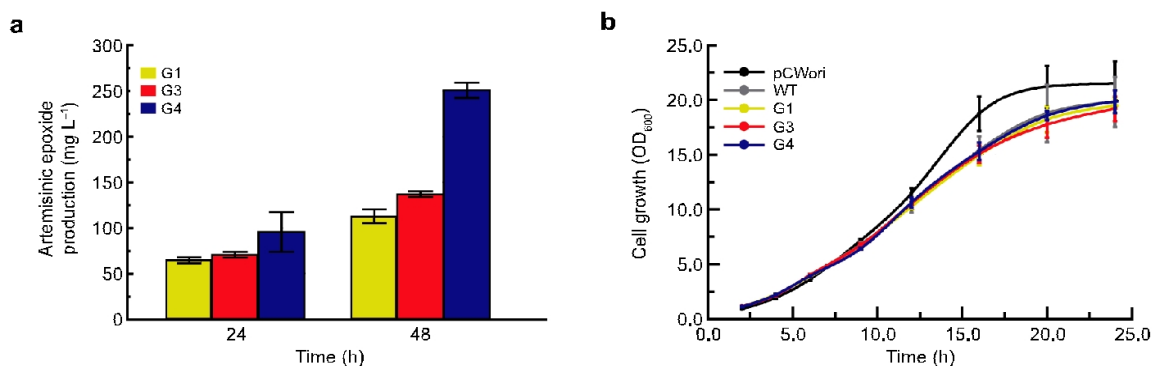


Figure 2. Improved *in vivo* production of artemisinic epoxide from P450_{BM3} variants. *E. coli* DH1 harboring pAM92 and a P450_{BM3} variant or the empty vector control plasmid pCWori was used for *in vivo* artemisinic epoxide production.

a) Production levels at 24 and 48 h post-inoculation.

b) Growth curves. (All data represent mean ± SD, n # 3.) Strains harboring pCWori or WT P450_{BM3} demonstrated no detectable production of artemisinic epoxide. No adverse physiological effects from P450_{BM3} overexpression or artemisinic epoxide production were observed, as demonstrated by the similar growth characteristics between all strains.

Product titers were quantified by comparison to a purified sample of microbially produced artemisinic epoxide of known concentration. P450_{BM3} variant G1 yielded 110 ± 8 mg L⁻¹ of artemisinic epoxide; as expected, variant G3 provided a modest improvement in production over G1, to levels of 140 ± 3 mg L⁻¹ (mean ± SD of triplicate measurements, Figure 2).

To investigate the possibility of further improving product titers, we selected four residues supported by our structure-based models in the P450_{BM3} active site on which saturation mutagenesis was performed. Position Phe87 was selected on the basis of previous results demonstrating a dramatic impact upon amorphadiene epoxidation. Positions Ile263, Ala264, and Ala328 were also selected; all three residues lie near the active site and

were believed to potentially affect substrate access to the prosthetic heme group. Using P450_{BM3} variant G3 as the starting template, each position was individually mutagenized, the resulting mutants were screened by sequencing for all possible amino acid mutations, and the resultant oxidized amorphadiene metabolite distribution and production of artemisinic epoxide for each mutant was analyzed by GC/MS (Supplementary Figure 3).

P450_{BM3} variants G3!A328L and G3!A328N were each identified to improve production of artemisinic epoxide by ~2.5-fold and ~3-fold over that of G3, respectively. Again, no other oxidized amorphadiene products were witnessed. Mutant variant G3!A328L (G4) demonstrated titers of artemisinic epoxide at levels greater than 250 ± 8 mg L⁻¹ following 48 h of culture (Figure 2). A structure-based interpretation of the active site mutations using ROSETTA-based energy minimization enabled a prediction of the amorphadiene epoxidation transition state complex (Figure 1). Introduction of mutation F87A opened up the active site and relieved the steric hindrance the phenylalanine residue imposed upon the ring structure of amorphadiene. Mutation A328L decreased the size of the P450_{BM3} binding pocket, restricting the mobility of amorphadiene and promoting access of the terminal olefin to the heme group of P450_{BM3} in the correct orientation.

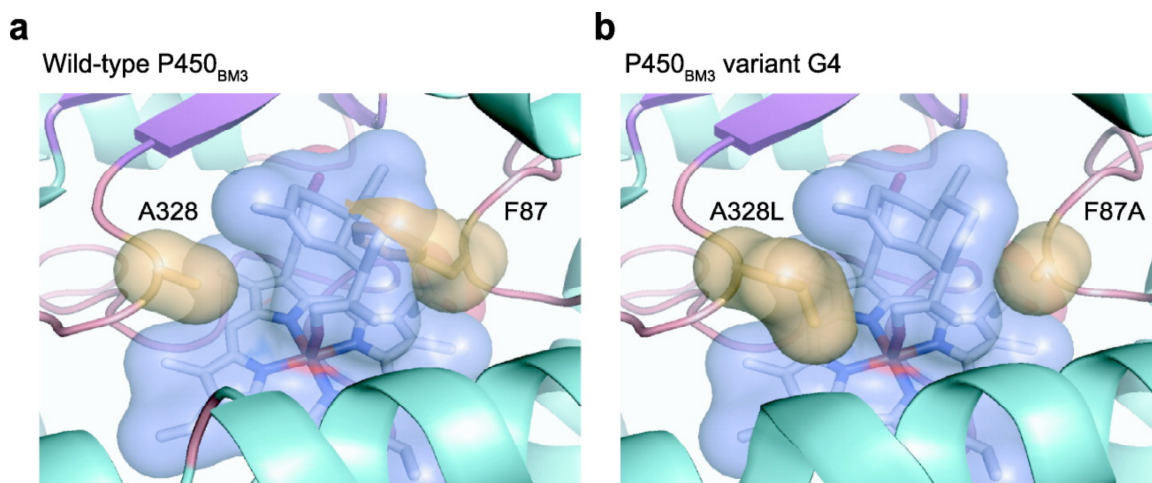


Figure 1. Transition state structures of active site mutations. Lowest energy transition state complexes were built using the Rosetta algorithm for both the wild-type (a) and mutated (b) active sites of P450_{BM3} with amorphadiene as a substrate. Mutation F87A appears to relieve the steric hindrance imposed upon amorphadiene and allows for increased access to the heme group. Mutation A328L appears to decrease the mobility of amorphadiene in the active site, promoting epoxidation.

Thus, the predicted transition state structures are in agreement with the observed *in vivo* production titers. The increase in terminal olefin epoxidation activity toward amorphadiene in variant G4 is in agreement with previous research showing that A328V increases terminal olefin epoxidation activity on linear hydrocarbons (29). Together, these results suggest a generalizable strategy for increasing epoxidation activity toward terminal alkenes in a broad range of structurally diverse substrates and deserve further exploration.

Of particular importance for *in vivo* expression of an engineered cytochrome P450 is the uncoupling of reduced NADPH consumption to oxidized products (e.g., superoxide radicals and hydrogen peroxide), resulting in increased oxidative stress. Engineered P450_{BM3} variants often exhibit extremely low coupling of NADPH to product formation (23, 24), potentially limiting the *in vivo* application of these engineered variants. To determine the extent to which decoupling could hinder *in vivo* performance, purified, wild-type P450_{BM3} and variants G1, G3, and G4 were incubated with amorphadiene, and NADPH consumption was monitored spectrophotometrically. Production of artemisinic epoxide was measured via GC/MS following complete consumption of NADPH, allowing the determination of uncoupling and amorphadiene oxidation rates (Table 1). Whereas the *in vitro* NADPH consumption rates between mutant variants followed a trend similar to the *in vivo* artemisinic epoxide production measurements, the amorphadiene oxidation rates plateau and incomplete conversion of added amorphadiene was witnessed. This finding suggests NADPH availability may be a limiting factor during *in vivo* production, a hypothesis supported by the observation that significant quantities of amorphadiene are also witnessed at the end points of the *in vivo* culture experiments. Increasing the *in vivo* NADPH supply to increase enzymatic activity has been successfully

employed in *E. coli* previously by increasing carbon flux through the pentose phosphate pathway (30, 31). A logical next step in improving artemisinic epoxide titers would explore this and other potential routes.

During *in vitro* experiments, all P450_{BM3} variants exhibited NADPH coupling efficiencies of approximately 50%, suggesting that amorphaadiene remains a difficult substrate for the studied P450_{BM3} variants to epoxidize. However, as exhibited by the growth curves (Figure 2), production of artemisinic epoxide did not appear to elicit adverse physiological effects. We believe differences in cell growth between P450_{BM3}-producing strains and the empty vector control were likely due to increased cell stress from P450_{BM3} overproduction.

The oxidation rate of palmitic acid with P450_{BM3} variant G4 was measured to estimate residual activity of our evolved P450 toward native fatty acid substrates. The palmitic acid oxidation rate was 154 ± 7 nmol (nmol P450) min⁻¹ (mean \pm SD, $n = 3$), compared to an oxidation rate of approximately 2,600 nmol (nmol P450)⁻¹ min⁻¹ for wild-type P450_{BM3} (22). Thus, there is a 15-fold decrease in activity toward a fatty acid substrate using the evolved mutant variant G4. However, the activity of variant G4 toward amorphaadiene is a fraction (86-fold less) of that of wild-type P450_{BM3} with fatty acid substrates. In light of this, further directed evolution of P450_{BM3} variant G4 is warranted and holds high potential to increase both substrate selectivity and activity toward amorphaadiene over fatty acid substrates.

In conclusion, production of artemisinin at low cost is highly dependent upon the capacity to successfully complete what is both relatively expensive and low-yielding synthetic chemistry (i.e., oxygenation and reduction) in a microbial host. Three selective oxidations at the terminal alkane and reduction of the terminal olefin are required for the conversion of amorphaadiene to dihydroartemisinic acid; conversion of dihydroartemisinic acid to artemisinin is well established (8, 9). Here, we present a novel route for the selective oxidation of amorphaadiene, yielding artemisinic-11S,12-epoxide at titers greater than 250 mg L⁻¹. Microbial production of artemisinic-11S,12-epoxide can be followed by a high-yielding synthetic chemistry route to dihydroartemisinic acid and onward to artemisinin. The strategy outlined here demonstrates improved production titers in *E. coli* compared to those previously achieved using the native P450_{AMO}-based pathway. Additionally, the P450_{BM3} route reduces culture time from 7 to 2 days, is optimal at 30 °C, and does not require reduction of the terminal olefin, as is the case when using P450_{AMO}. Thus, the strategy outlined here is a viable alternative to the native P450_{AMO}-catalyzed route. This semi-biosynthetic approach outlines a metabolic engineering paradigm for pathway design based on incorporation of enzymes with broad substrate promiscuity that can be well expressed in a heterologous host. In contrast to previous works with P450_{BM3}, in which mutations are introduced randomly or based on crystal structures of native substrate-bound P450_{BM3}, transition state complex modeling with amorphaadiene greatly improved our ability to select a minimum number of active site residues for mutation. The model provided both a rationale for selecting residues and putative explanations for observed changes in activity. The use of transition state complex structural predictions is a highly robust approach that improves upon our ability to rationally redesign promiscuous enzymes and tailor them toward specific applications in metabolic engineering.

METHODS

Reagents and Equipment.

All enzymes and chemicals were purchased from New England Bio-labs and Sigma-Aldrich Co., respectively, unless otherwise indicated. Gas chromatography was conducted on a Polaris Q (Thermo Electron Corporation) gas chromatograph, a DB5 capillary column (30 m \times 250 μ m internal diameter, 0.25 μ m film thickness, Agilent), and a TriPlus auto sample-injector (Thermo Electron Corporation). ¹H NMR spectra were collected in CDCl₃ (Cambridge Isotope Laboratories) at 25 °C on a Bruker AV-500 or AV-400 spectrometer at the University of California at Berkeley, College of Chemistry NMR Facility.

Transition State Complex Structural Predictions.

The transition state complex for the epoxidation of amorpha-4,11-diene was constructed on the basis of previously performed energy density calculations on propene hydroxylation and epoxidation (32). ROSETTA-based energy minimization was carried out based on previously described methodologies (33). The resulting model was visualized using PYMOL (34).

Purification of P450_{BM3} Variants.

DH1 strains harboring a pT_{rc}SBM3-15 variant (WT, G1, G3, G4) were inoculated into 5 mL of Terrific Broth (TB) containing Cb⁵⁰ and grown overnight at 30 °C. Next, 500 mL of fresh TB containing Cb⁵⁰ was inoculated using the overnight cultures to an optical density at a wavelength of 600 nm (OD₆₀₀) of 0.05 and grown at 30 °C. Approximately 1 h prior to induction, cultures were further supplemented with 65

mg L⁻¹ ALA. Upon reaching an OD₆₀₀ of 0.60, cultures were induced with 0.05 mM IPTG and grown for an additional 15 h. Cultures were then centrifuged (5000 'g, 4 °C, 15 min) and resuspended in 10 mL of S-tag purification kit (Novagen) wash/bind buffer containing 20 U of Dnase I and bacterial protease inhibitor. The suspension was then sonicated (VirTis) on ice and centrifuged (15000 'g, 4 °C, 15 min), and the resulting supernatant was passed through a 0.45 µm filter. S-tag purification was used following the recommended protocol with the exception that the thrombin cleavage step was extended to 4 h. The eluted protein was concentrated using a centrifugal spin filter (Millipore, MWCO 10,000). P450_{BM3} concentration was measured by its carbon monoxide difference spectra (35).

In Vitro P450_{BM3} Characterization.

The NADPH turnover rate was determined by incubation of a purified P450_{BM3} variant in the presence of amorphaadiene or palmitic acid and NADPH. A 1-mL reaction volume containing 1 µM purified P450_{BM3} and 500 µM substrate in 100 mM potassium phosphate buffer (pH 7.5) was equilibrated to 30 °C. To initiate the reaction, 250 µM NADPH was added to the solution, and the absorbance at 340 nm was monitored. NADPH turnover rates were calculated with $\epsilon_{340} = 6.22 \text{ mM}^{-1} \text{ cm}^{-1}$.

For amorphaadiene samples, following complete consumption of NADPH, 900 µL of the reaction volume was taken and added to 500 µL of ethyl acetate containing 50 µg mL⁻¹ caryophyllene for use as the internal standard in GC/MS analysis. The mixture was vortexed and centrifuged (5000 'g, 25 °C, 1 min), and the organic layer was sampled. Samples were then analyzed by GC/MS using the method indicated previously.

Coupling of NADPH turnover to epoxidation of amorphaadiene was calculated by measuring the decrease in amorphaadiene peak area. The apparent initial rate of amorphaadiene epoxidation was then obtained by multiplying the coupling efficiency by the NADPH consumption rate. For palmitic acid samples, 500 µL of the reaction volume was derivatized with 20 µL of 2 M TMS-diazomethane and 50 µL of 10% methanol.

The reactions were allowed to proceed for 30 min at RT and quenched with 5 µL of acetic acid. The samples were then analyzed by GC/MS using the previously described method. Coupling of NADPH turnover to hydroxylation of palmitic acid was calculated by measuring the decrease in palmitic acid peak area. The apparent initial rate of palmitic acid hydroxylation was then obtained by multiplying the coupling efficiency by the NADPH consumption rate.

In Vivo Production, Purification, and Chemical Analysis of Artemisinic-11S,12-epoxide.

Precultured *E. coli* DH1 transformed with pAM92 and either a pTrcBM3-14 or pCWoriBM3 variant (pTRC for initial screening assays and pCWori for final production assays) was inoculated into fresh TB supplemented with 2% glycerol (v/v), 65 mg L⁻¹ aminolevulinic acid hydrochloride (ALA), and 50 µg mL⁻¹ each of carbenicillin (Cb⁵⁰) and chloramphenicol (Cm⁵⁰). All cultures were inoculated at an OD₆₀₀ of 0.05. Cultures were induced with IPTG (0.05 mM with pTRC and 1 mM with pCWori) upon reaching an OD₆₀₀ of 0.25. After 24 and 48 h of culture at 30 °C, 250 µL of culture was extracted with 750 µL of ethyl acetate spiked with caryophyllene (150 µg mL⁻¹) as an internal standard. The organic layer was then sampled and analyzed by GC/MS (70 eV, Thermo Electron) equipped with a DB5 capillary column (30 m × 0.25 mm internal diameter, 0.25 µm film thickness, Agilent Technologies). The gas chromatography program used was 100 °C for 5 min, then ramping 30 °C min⁻¹ to 150 °C, 5 °C min⁻¹ to 180 °C, and 50 °C min⁻¹ to 300 °C. Identification and quantification of microbially produced artemisinic-11S,12-epoxide was carried by GC/MS using authentic artemisinic epoxide standards (obtained from Amyris Biotechnologies) of known concentration. ¹H NMR spectroscopy was used to confirm the GC/MS identification (Supplementary Figure 2).

Experimental Determination of Microbially Produced Artemisinic-11S,12-epoxide Stereochemistry.

DH1 strains harboring pAM92 and pTrcBM3-14 (G4) used in production assays were extracted into an equal volume of ethyl acetate. After drying, the crude epoxide was purified by silica gel chromatography using 5% ethyl acetate in hexanes as eluent. The mixture was dried *in vacuo*, yielding impure epoxide (5.6 mg, ca. 75% pure, 0.019 mmol, contains amorphaadiene). The mixture was dissolved in 0.40 mL of tetrahydrofuran, and solid sodium cyanoborohydride (27.4 mg, 0.44 mmol) was added, followed by 5 mL of bromocresol green indicator solution. Five drops of 0.15 mL of boron trifluoride in 1.0 mL of tetrahydrofuran was added, causing the blue color to discharge. After 112 h of stirring, an additional

portion of sodium cyanoborohydride (26.6 mg, 0.423 mmol) was added, followed by an additional 5 mL of the indicator, followed by 5 drops of the boron trifluoride solution. The mixture was stirred an additional 48 h and then dried *in vacuo*. The residue was dissolved in a mixture of 1 mL of ethyl acetate and 1 mL of water. The layers were separated, and the organic phase was concentrated. The oil was purified by silica gel chromatography using 10% ethyl acetate as eluant to give 2.7 mg of recovered epoxide, along with 2.2 mg of dihydroartemisinic alcohol (39% yield, or 81% based on recovered epoxide). Stereochemistry of the purified dihydroartemisinic alcohol was confirmed to be (*R*) by comparison to published

¹H NMR results (25). Hydride attack to produce the (*R*) stereochemistry of the alcohol under these conditions necessitates that artemisinic-11*S*,12-epoxide be the substrate (36).

Competing Interest Statement: J.K. is a founder of and has a financial interest in Amyris. Amyris will not make any profit from the production or sale of artemisinin, and the University of California will not receive any royalties for any licenses to any artemisinin production process.

Acknowledgment: This research was conducted under the sponsorship of the Institute for OneWorld Health, through the generous support of The Bill and Melinda Gates Foundation. Y.Y. acknowledges a postdoctoral fellowship from the Jane Coffin Childs Memorial Fund. We thank J. C. Fortman and M. Ouellet for advice in purification and mass spectrometry. *

Supporting Information Available: This material is available free of charge via the Internet at <http://pubs.acs.org>.

REFERENCES

1. Jensen, R. A. (1976) Enzyme recruitment in evolution of new function, *Annu. Rev. Microbiol.* 30, 409–425.
2. Khersonsky, O., Roodveldt, C., and Tawfik, D. S. (2006) Enzyme promiscuity: evolutionary and mechanistic aspects, *Curr. Opin. Biotechnol.* 10, 498–508.
3. Hult, K., and Berglund, P. (2007) Enzyme promiscuity: mechanism and applications, *Trends Biotechnol.* 25, 231–238.
4. Olumeses, P. (2006) *Guidelines for the Treatment of Malaria*, World Health Organization, Geneva.
5. Hale, V., Keasling, J. D., Renninger, N., and Diagana, T. T. (2007) Microbially derived artemisinin: a biotechnology solution to the global problem of access to affordable antimalarial drugs, *Am. J. Trop. Med. Hyg.* 77, 198–202.
6. Korenromp, E., Miller, J., Nahlen, B., Wardlaw, T., and Young, M. (2005) *World Malaria Report 2005*, World Health Organization, Roll Back Malaria, Geneva.
7. Covello, P. S. (2008) Making artemisinin, *Phytochemistry* 69, 2881–2885.
8. Acton, N., and Roth, R. J. (1992) On the conversion of dihydroartemisinic acid into artemisinin, *J. Org. Chem.* 57, 3610–3614.
9. Haynes, R. K., and Vonwiller, S. C. (1994) Cyclic per-oxyacetal lactone, lactol and ether compounds, *U.S. Patent 5310946*.
10. Martin, V. J. J., Pitera, D. J., Withers, S. T., Newman, J. D., and Keasling, J. D. (2003) Engineering a mevalonate pathway in *Escherichia coli* for production of terpenoids, *Nat. Biotechnol.* 21, 796–802.
12. Newman, J. D., Marshall, J., Chang, M., Nowroozi, F., Paradise, E., Pitera, D., Newman, K. L., and Keasling, J. D. (2006) High-level production of amorpha-4,11-diene in a two-phase partitioning bioreactor of metabolically engineered *Escherichia coli*, *Biotechnol. Bioeng.* 95, 684–691. Pitera, D. J., Paddon, C. J., Newman, J. D., and Keasling, J. D. (2007) Balancing a heterologous mevalonate pathway for improved isoprenoid production in *Escherichia coli*, *Metab. Eng.* 9, 193–207.

*Work was also supported by the U.S. Department of Energy under Contract No. DE-AC02-05CH11231.

13. Ro, D.-K., Paradise, E. M., Ouellet, M., Fisher, K. J., Newman, K. L., Ndungu, J. M., Ho, K. A., Eachus, R. A., Ham, T. S., Kirby, J., Chang, M. C. Y., Withers, S. T., Shiba, Y., Sarpong, R., and Keasling, J. D. (2006) Production of the antimalarial drug precursor artemisinic acid in engineered yeast, *Nature (London)* 440, 940–943.
14. Reiling, K. K., Renninger, N. S., McPhee, D. J., Fisher, K. J., and Ockey, D. A. (2006) Conversion of amorpha-4,11-diene to artemisinin and artemisinin precursors, *U.S. Patent Application 20060270863*.
15. Schmid, A., Dordick, J. S., Hauer, B., Kiener, A., Wubbolts, M., and Witholt, B. (2001) Industrial biocatalysis today and tomorrow, *Nature (London)* 409, 258–268.
16. Schoemaker, H. E., Mink, D., and Wubbolts, M. G. (2003) Dispelling the myths "biocatalysis in industrial synthesis", *Science* 299, 1694–1697.
17. Carter, O. A., Peters, R. J., and Croteau, R. (2003) Monoterpene biosynthesis pathway construction in *Escherichia coli*, *Phytochemistry* 64, 425–433.
18. Chang, M. C. Y., Eachus, R. A., Trieu, W., Ro, D.-K., and Keasling, J. D. (2007) Engineering *Escherichia coli* for production of functionalized terpenoids using plant P450s, *Nat. Chem. Biol.* 3, 274–277.
19. Thomas, A. F., and Bessiere, Y. (1989) Limonene, *Nat. Prod. Rep.* 6, 291–309.
20. Bhyrappa, P., Young, J. K., Moore, J. S., and Suslick, K. S. (1996) Dendrimer-metalloporphyrins: synthesis and catalysis, *J. Am. Chem. Soc.* 118, 5708–5711.
21. Noble, M. A., Miles, C. S., Chapman, S. K., Lysek, D. A., MacKay, A. C., Reid, G. A., Hanzlik, R. P., and Munro, A. W. (1999) Roles of key active-site residues in flavocytochrome P450 BM3, *Biochem. J.* 339, 371–379.
22. Glieder, A., Farinas, E. T., and Arnold, F. H. (2002) Laboratory evolution of a soluble, self-sufficient, highly active alkane hydroxylase, *Nat. Biotechnol.* 20, 1135–1139.
23. Carmichael, A. B., and Wong, L.-L. (2001) Protein engineering of *Bacillus megaterium* CYP102. The oxidation of polycyclic aromatic hydrocarbons, *Eur. J. Biochem.* 268, 3117–3125.
24. Sowden, R. J., Yasmin, S., Rees, N. H., Bell, S. G., and Wong, L.-L. (2005) Biotransformation of the sesqui-terpene (1)-valencene by cytochrome P450_{ca} and P450_{BM3}, *Org. Biomol. Chem.* 3, 57–64.
25. Berteau, C. M., Freije, J. R., van der Woude, H., Verstappen, F. W. A., Perk, L., Marquez, V., De Kraker, J.-W., Posthumus, M. A., Jansen, B. J. M., de Groot, A., Franssen, M. C. R., and Bouwmeester, H. J. (2005) Identification of intermediates and enzymes involved in the early steps of artemisinin biosynthesis in *Artemisia annua*, *Planta Med.* 71, 40–47.
- Wallaart, T. E., van Uden, W., Lubberink, H. G. M., Woerdenbag, H. J., Pras, N., and Quax, W. J. (1999) Isolation and identification of dihydroartemisinic acid from *Artemisia annua* and its possible role in the biosynthesis of artemisinin, *J. Nat. Prod.* 62, 430–433
27. Simons, K. T., Kooperberg, C., Huang, E., and Baker, D. (1997) Assembly of protein tertiary structures from fragments with similar local sequences using simulated annealing and bayesian scoring functions, *J. Mol. Biol.* 268, 209–225.
28. Ost, T. W. B., Miles, C. S., Murdoch, J., Cheung, Y.-F., Reid, G. A., Chapman, S. K., and Munro, A. W. (2000) Rational re-design of the substrate binding site of flavocytochrome P450 BM3, *FEBS Lett.* 486, 173–177.
29. Kubo, T., Peters, M. W., Meinhold, P., and Arnold, F. H. (2006) Enantioselective epoxidation of terminal alkenes to (R)- and (S)-epoxides by engineered cytochromes P450 BM-3, *Chem. Eur. J.* 12, 1216–1220.
- Lim, S.-J., Jung, Y.-M., Shin, H.-D., and Lee, Y.-H. (2002) Amplification of the NADPH-related genes

- zwf and gnd for the oddball biosynthesis of PHB in an *E. coli* transformant harboring a cloned phbCAB operon, *J. Biosci. Bioeng.* 93, 543–549.
31. Lee, W.-H., Park, J.-B., Park, K., Kim, M.-D., and Seo, J.-H. (2007) Enhanced production of ϵ -caprolactone by overexpression of NADPH-regenerating glucose 6-phosphate dehydrogenase in recombinant *Escherichia coli* harboring cyclohexanone monooxygenase gene, *Appl. Microbiol. Biotechnol.* 76, 329–338.
33. de Visser, S. P. (2006) What factors influence the ratio of C-H hydroxylation versus CAC epoxidation by a nonheme cytochrome P450 biomimetic? *J. Am. Chem. Soc.* 128, 15809–15818 Zanghellini, A., Jiang, L., Wollacott, A. M., Cheng, G., Meiler, J., Althoff, E. A., Rothlisberger, D., and Baker, D. (2006) New algorithms and an in silico benchmark for computational enzyme design, *Protein Sci.* 15, 2785–2794.
34. DeLano, W. L. (2002) The PyMOL molecular graphics system, <http://www.pymol.org>.
35. Omura, T., and Sato, R. (1964) The carbon monoxide-binding pigment of liver microsomes. I. Evidence for its hemoprotein nature, *J. Biol. Chem.* 239, 2370–2378.
36. Hutchins, R. O., Taffer, I. M., and Burgoyne, W. (1981) Regio- and stereoselective cleavage of epoxides with cyanoborohydride and boron trifluoride etherate, *J. Org. Chem.* 46, 5214–5215.